Article

Dehydrogenation of Ethanol to Acetaldehyde over Co/C Catalysts

Jeerati Ob-eye and Bunjerd Jongsomjit[*]

Center of Excellence on Catalysis and Catalytic Reaction Engineering, Department of Chemical Engineering, Faculty of Engineering, Chulalongkorn University, Bangkok 10330, Thailand
E-mail: jijeejaa@hotmail.com, [*]bunjerd.j@chula.ac.th (Corresponding author)

Abstract. This study focuses on the production of acetaldehyde from ethanol by catalytic dehydrogenation using Co/C catalysts with different Co loading on the activated carbon derived from coffee ground residues. The simple impregnation was used to obtain the Co/C catalysts having Co loading of ca. 4 and 6 wt%. The catalysts were characterized using various techniques. The dehydrogenation of vaporized ethanol was conducted in order to measure the catalytic activity and product distribution at temperatures ranging from 250 to 400°C. Based on this study, it appeared that the Co/C catalyst having ca. 4 wt% of cobalt loading (4%Co/C) exhibited the highest ethanol conversion (54%) at 400°C with the acetaldehyde yield of 50%. In addition, all catalysts behaved similar catalytic properties, where the ethanol conversion increased with increasing the reaction temperature having acetaldehyde as a major product. The high activity obtained from 4%Co/C and C catalysts can be remarkably attributed to the high acidity to basicity (~1.50). Hence, the 4%Co/C is promising catalyst for ethanol dehydrogenation to acetaldehyde.

Keywords: Ethanol dehydrogenation, cobalt, activated carbon.

1. Introduction

Ethanol is considered as a promising renewable raw material to possibly produce many chemical feedstocks including ethylene, diethyl ether, acetaldehyde, etc. The reactions of ethanol on catalytic materials have been continuously investigated for more than three decades [1-3]. These studies have been motivated by the more effectiveness of ethanol utilization, especially when ethanol is abundant due to the less usage of ethanol in fossil fuels. One of the most encouraging strategies is to add value to ethanol by converting it into other chemicals. A wide range of intermediates, large-scale end products, such as bulk and fine chemicals, including ethylene, hydrogen, ethyl acetate, acetaldehyde, acetic acid, carbon monoxide, aromatic hydrocarbons, and other compounds, can in principle be synthesized from ethanol. Among these chemicals, acetaldehyde is one of the attractive chemicals, which is produced and consumed globally for different industrial applications. The market for acetaldehyde is primarily expected to be driven by the downstream markets that use the compound as a key raw material [4]. Acetic acid, acetic anhydride, n-butanol, and 2-ethylhexanol are the major products derived from acetaldehyde. The commercial production processes of acetaldehyde include dehydrogenation and oxidation of ethanol, the hydration of acetylene, the partial oxidation of hydrocarbons, and direct oxidation of ethylene.

With the ever-growing of the world output of bioethanol, the production of acetaldehyde via dehydrogenation of ethanol is interesting. The properties of catalysts used to catalyze the ethanol reaction, have a great influence to the pathway mechanism project to the desire products. If the aspire product is acetaldehyde, catalysts often containing many metals such as Cu, Cr or Zn are promising [3, 5-6]. Cobalt catalysts has been used in many reaction [7-8]. Meanwhile, only few literatures use cobalt metal catalyst in ethanol dehydrogenation [9-11]. Church *et al.* [12] used cobalt metal as a promoter on copper catalyst. Results found that high ethanol conversion of 94% with acetaldehyde yield of 84% were obtained, whereas only 79% of ethanol conversion and acetaldehyde yield of 71% at 330°C were observed in the absence of cobalt metal. Zhou *et al.* [13] applied cobalt on octahedral molecular sieve catalyst, it showed that ethanol conversion ca. 63% and 45% of acetaldehyde yield at 300°C were obtained in oxidative ethanol dehydrogenation reaction, while with the absence of cobalt promoter, the ethanol conversion of 56% and acetaldehyde yield of 36% at same temperature were found. Moreover, Ashok *et al.* [9] used cobalt nanoparticles via solution combustion synthesis for ethanol dehydrogenation, which resulted in high selectivity for acetaldehyde and acetate. It was an interesting report by Sales *et al.* [14] who employed the bimetallic Co-Cu on carbon catalyst that showed surface area of 986 m^2/g, ethanol conversion about 78.5% at 400°C in oxidative ethanol dehydrogenation reaction. Without cobalt modification, it exhibited only 74% of ethanol conversion at same temperature. In addition, cobalt-exchanged zeolites also showed higher hydrothermal stability than copper-exchanged zeolites, maintaining high N2O decomposition activity [11]. This study highlighted on the utilization of cobalt doped on carbon catalyst to produce acetaldehyde by ethanol dehydrogenation reaction.

As biomass derived material, activated carbon is very captivating because it can be used as a catalyst or a catalyst support in many catalytic processes [10, 15]. In fact, activated carbon can be synthesized from a variety of carbonaceous source materials. In practice, coal and many agricultural biomass byproducts are commonly used as raw materials to produce commercial activated carbons. There are many studies relating to the preparation and characterization of activated carbons from agricultural wastes [16-20]. However, it has been perhaps only a few publications reporting on the preparation of effective activated carbon catalyst from coffee ground residues. Therefore, this feasibility study was carried out to determine the use of coffee ground residues to prepare highly effective activated carbon catalysts, especially for gaseous reaction.

In this present work, the coffee residue-derived activated carbon-supported cobalt catalysts (Co/C) was prepared with varying Co loading (ca. 4 and 6 wt%) and characterized with various characterization techniques. Then, the catalysts were tested for ethanol dehydrogenation in a micro packed-bed reactor under temperature-programmed reaction from 250 to 400°C. The ethanol conversion and product selectivity obtained from different catalysts were measured. The relationship between physicochemical properties and catalytic properties will be discussed further.

2.   Materials and Methods

2.1. Raw Materials and Chemicals

The coffee residues used as the raw material to produce the activated carbon in this study were obtained from Starbucks Thailand.

The chemicals used were as follows: zinc chloride (>98% $ZnCl_2$; Aldrich), hydrochloric acid (37% HCl; QReC), distilled water, cobalt (II) nitrate hexahydrate 98+%, 99% nitrogen gas and 99% carbon dioxide gas.

2.2. Preparation of Activated Carbons

First, the coffee residue was washed with distilled water and dried at 110°C for 24 h. After cooling, the dried coffee residue was mixed with $ZnCl_2$ with a mass ratio of coffee residue to $ZnCl_2$ of 1:3 and dried in an oven at 110°C for 24 h. The mixture was activated under N_2 by heating from room temperature to 600°C followed by hold at that temperature under CO_2 atmosphere for 4 h with a heating rate of 10°C/min, and then cool down to the room temperature under N_2 flow. The samples were washed with 1M HCl, and followed several washed with distilled water. Finally, they were dried at 110°C for 24 h. The desired amounts of cobalt (II) nitrate hexahydrate were used in order to have the Co loading of 4 and 6 wt% in the final catalysts as shown in Table 2. Deionized water was used as a solvent having its volume equals to pore volume of catalyst. Then, the aqueous solution of cobalt was slowly impregnated onto activated carbons. The samples were dried in an oven at 110°C for 24 h. Finally, the catalysts were calcined in N_2 at 350°C for 6 h.

2.3. Characterization of Activated Carbons

The surface area, pore volume, and pore diameter of the activated carbon were measured by N_2 adsorption-desorption at liquid nitrogen temperature (-196°C) using a Micromeritics ASAP 2020 analyzer. The surface area and pore distribution were calculated according to the BET and BJH methods, respectively.

X-ray diffraction (XRD) was performed to determine crystalline structures of activated carbon and raw material using a Siemens D 5000 X-ray diffractometer having CuK_α radiation with Ni filter in the 2θ range of 10–80 with a resolution of 0.04.

Scanning electron microscopy (SEM; JEOL model JSM-5800LV) and energy dispersive X-ray spectroscopy (EDX) were used to determine the morphology and elemental distribution of catalysts. Model of SEM: JEOL mode JSM-5800LV was used and EDX was performed using Link Isis Series 300 program.

Transmission electron microscopy (TEM; JEOL JEM-2010) was used to determine the morphology and size of metal on the catalyst with thermionic electron type LaB_6 as a source, operating at 200 kV.

Temperature-programmed desorption of carbon dioxide (CO_2-TPD) was performed using Micromeritics Chemisorp 2750 automated system to study the basic properties. In the study, 0.05 g of catalyst was packed in a U-tube quartz cell with 0.03 g of quartz wool and pretreated at 500°C under helium flow rate 25 cm^3/min for 1 h. The catalyst sample was saturated with CO_2 at ambient temperature for 30 min. Then, the physisorbed CO_2 on the catalyst surface was removed by the He flow rate of 25 cm^3/min for 15 min. After that, the temperature-programmed desorption was carried out from 40°C to 500°C at heating rate of 10°C/min. The amount of CO_2 in effluent gas was analyzed via thermal conductivity detector (TCD) as a function of temperature.

Temperature-programmed desorption of ammonia (NH_3-TPD) was performed using Micromeritics Chemisorp 2750 automated system to study the acid properties. In the study, 0.05 g of catalyst was packed in a U-tube quartz cell with 0.03 g of quartz wool and pretreated at 500°C under helium flow rate 25 cm^3/min for 1 h. The catalyst sample was saturated with NH_3 at ambient temperature for 30 min. Then, the physisorbed NH_3 on the catalyst surface was removed by the He flow rate 25 cm^3/min for 15 min. After that, the temperature programmed desorption was carried out from 40°C to 500°C at heating rate 10°C/min. The amount of NH_3 in effluent gas was analyzed via thermal conductivity detector (TCD) as a function of temperature.

The Fourier transform infrared (FTIR) spectrometry was applied in the characterization of the functional groups of the activated carbon prepared. To obtain the observable absorption spectra, it was performed using Nicolet 6700 FTIR spectrometer in the range of 400 to 4000 cm^{-1}.

Thermogravimetric analysis (TGA) was performed using an SDT Analyzer Model Q600 from TA Instruments (USA). The TGA analyses of the activated carbon were carried out from room temperature to 900°C at a heating rate of 10°C/min under nitrogen atmosphere at the flow rate of 100 ml/min.

Inductively coupled plasma mass spectrometer (ICP) was used to determine the actual amount of the metal loading.

2.4. Catalytic Activity with Ethanol Dehydrogenation

The similar ethanol reaction (temperature-programmed reaction) system as reported by Krutpijit *et al.* and Kumsuwan *et al.* [21, 22] was used. The catalytic dehydrogenation of ethanol was performed in the fixed-bed continuous flow microreactor. First, 0.05 g of catalyst and 0.01 g of quartz wool bed were packed in the middle of glass tube reactor, which is located in the electric furnace. Before the reaction was carried out, catalyst was preheated at 200°C for 30 min in nitrogen to remove the moisture. Then, the catalyst was reduced at 400°C for 3 h by hydrogen gas flow. The liquid ethanol was vaporized at 120°C with nitrogen gas (60 ml/min) by controlled injection with a single syringe pump at a constant flow rate of ethanol at 1.45 ml/h. The gas stream was introduced to the reactor with the weight hourly space velocity (WHSV) of 22.9 $g_{ethanol}g_{cat}^{-1}h^{-1}$ and the reaction was carried out at temperature range from 250°C to 400°C under atmospheric pressure. The gaseous products were analyzed by a Shimadzu (GC-14B) gas chromatograph with flame ionization detector (FID) using capillary column (DB-5) at 150°C. Upon the reaction test, at least three times for each sampling were recorded. The average values for ethanol conversion and product distribution as a function of temperature were reported.

3. Results and Discussion

3.1. Catalysts Characterization

Table 1 shows the BET surface areas, pore volume and pore size diameter of Co/C catalysts. Other structural parameters obtained from the N_2 adsorption-desorption are also summarized in Table 1. Data are tabulated for BET surface area, total pore volume, micropore volume, average pore width, and the ratio of micropore volume to total pore volume (% microporosity). The C catalyst exhibited the highest BET surface area and total pore volume. When the amount of cobalt metal loading increased, the BET surface area and the total pore volume of catalysts apparently decreased. This indicated that the pore blockage by cobalt clusters evidently occurred.

The characteristics of adsorption-desorption isotherms are effectively used to identify the type of pores characteristics of catalyst samples. The N_2 adsorption-desorption isotherms of all catalysts are shown in Fig. 1. The isotherms of the activated carbons exhibit a combination of types I (major) and IV (minor) according to the IUPAC [23]. A combination of types I and IV isotherms are usually indicated the presence of both microporous and mesoporous structure. The isotherms display a sharply increase in N_2 adsorption in the initial relative pressure range indicating the formation of micropores. In addition, the isotherms also appear to contain hysteresis loop at high relative pressure suggesting that the pore structure is partly mesopores. So, the activated carbons with different cobalt loadings have both microporous and mesoporous structures. The adsorption capacity is at a maximum of the C catalyst showing that the pore volume has the maximum amount at this sample. While the C catalyst has 100% of micropore volume and smallest pore size.

Table 1. Surface areas and pore characteristics for Co/C catalysts.

Catalysts	C	4%Co/C	6%Co/C
S_{BET} (m²/g)	1,037	727	683
V_t (cm³/g)	0.49	0.36	0.35
V_{mic} (cm³/g)	0.49	0.35	0.33
% V_{mic}	100	98.83	92.70
D_p (nm)	1.87	1.96	2.07

S_{BET}, BET surface area; V_t, total pore volume; V_{mic}, micropore volume; %V_{mic}, (V_{mic}/V_t) x 100; Dp, average pore diameter calculated as 4V/A by BET.
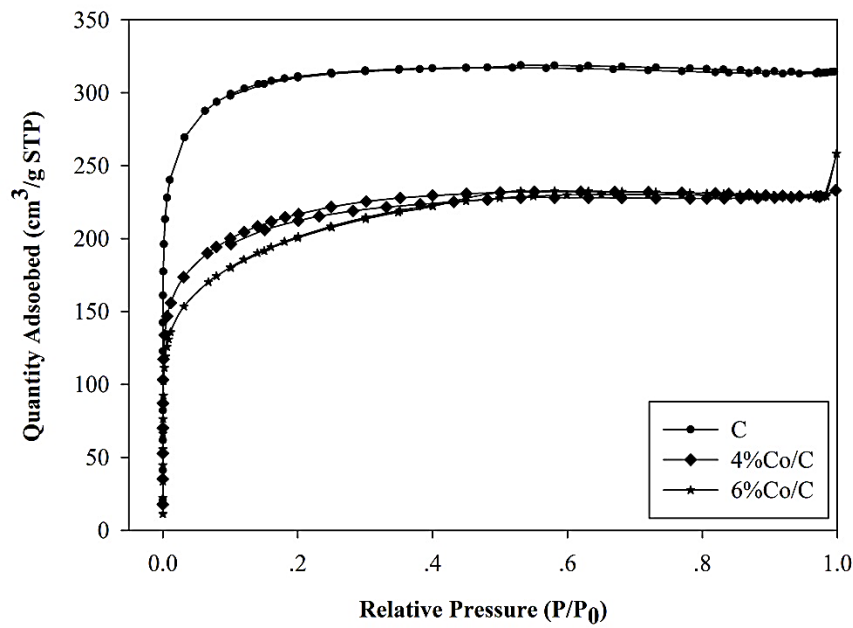
Fig. 1.   Adsorption-desorption isotherm at -196oC of activated carbon-supported Co catalysts.
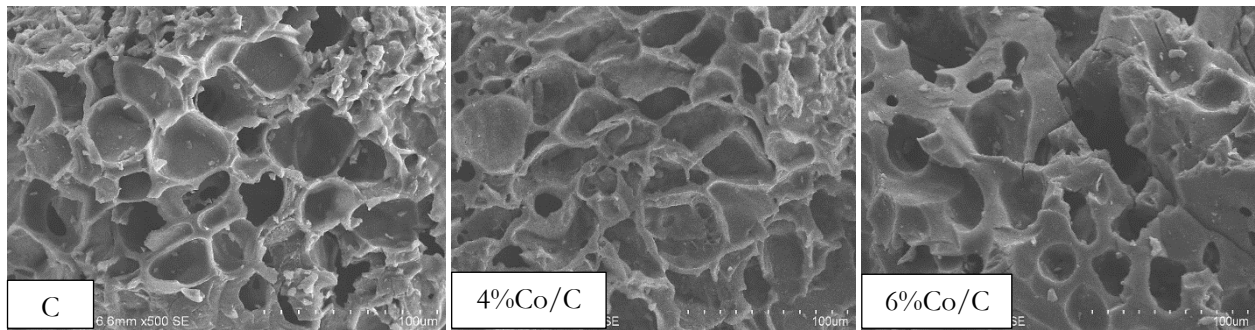

Fig. 2.   SEM images of activated carbon-supported Co catalysts.

Scanning electron microscopy (SEM) was conducted in order to study the morphologies of the samples. From Fig. 2, it was found that all catalysts exhibited high porosity. The C and 4%Co/C catalysts has a uniformly porous structure. With 6% of Co impregnated, the agglomeration occured due to cobalt blocked of carbon substrate.

Table 2.   %Co content of the carbon-supported Co catalysts.

Activated carbons	% wt Co*a	% wt Co*b
4% Co/C	4.2	17.06
6% Co/C	6.2	31.38

*a by ICP
*b by EDX
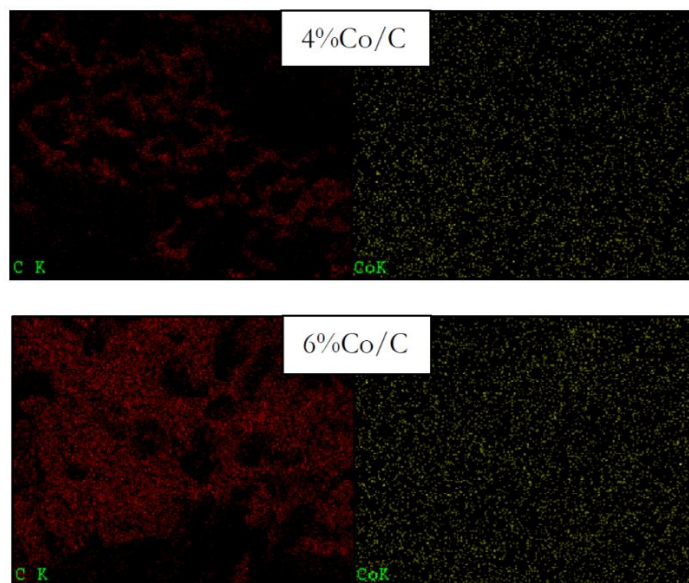
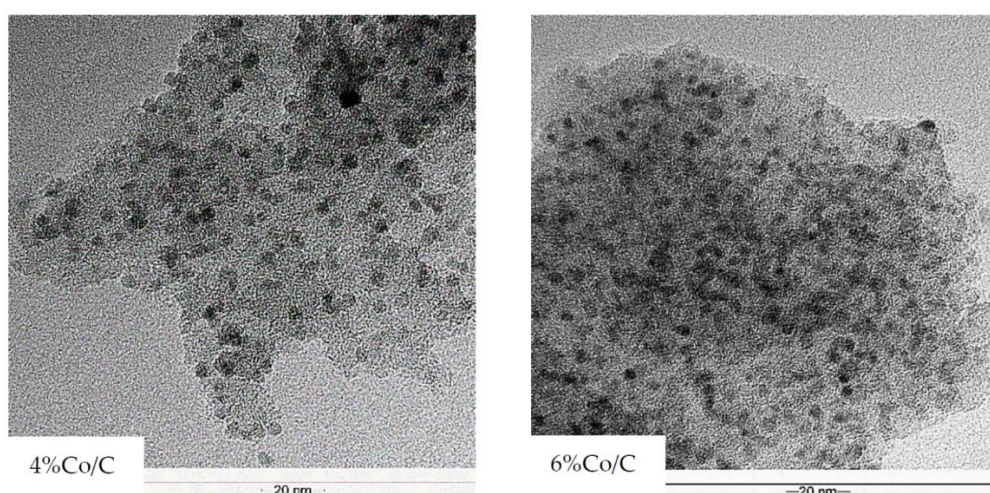Fig. 3.   EDX of activated carbon-supported Co catalysts.

Fig. 4.   TEM images of activated carbon-supported Co catalysts.

The results of Co content for the catalyst samples are illustrated in Table 2. Results found that Co content on surface of catalysts was higher than that in bulk of catalysts. This was probably due to particle size of Co metal is larger than the pore size of catalysts. Energy dispersive X-ray spectroscopy (EDX) was performed in order to study cobalt distribution (as displayed in Fig. 3). On the right hand side, the yellow dots represent the distribution of cobalt metal. In addition, TEM micrographs of activated carbon-supported Co catalysts are shown in Fig. 4. For cobalt catalysts, the dark patches represent the cobalt species dispersing on all catalysts. It revealed that with larger amount of Co loading, the Co species started to agglomerate (6%Co/C). Both techniques showed that cobalt species of 6%Co/C were located mostly on the external surface as seen by EDX with some agglomeration.

Table 3.   Total acidity and total basicity of carbon-supported Co catalysts.

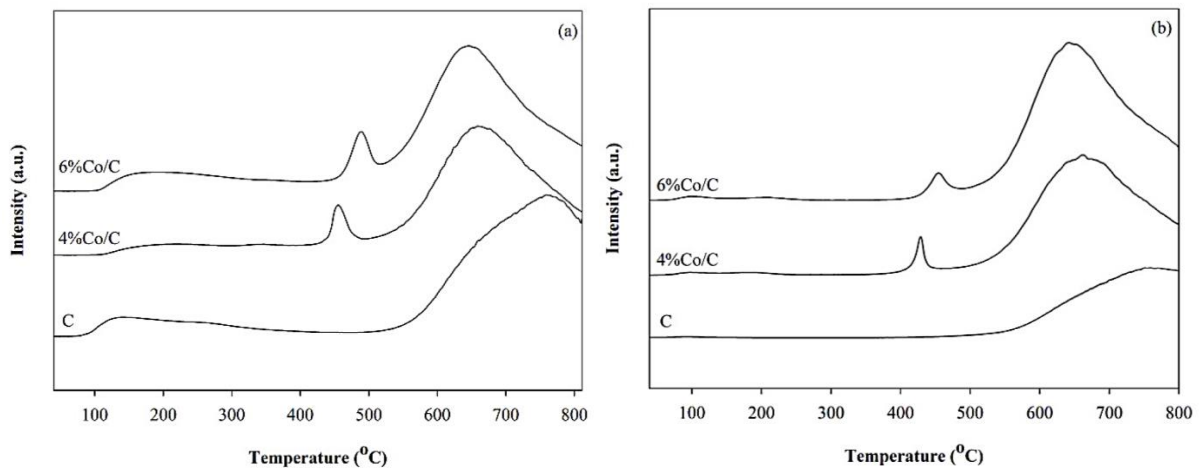| Activated carbons	Total acidity[a] (µmol/g)	Total basicity[b] (µmol/g)	Acidity/basicity
C	577.4	383.7	1.50
4%Co/C	244.3	161.3	1.51
6%Co/C	213.8	155.0	1.38

[a] NH_3-TPD, [b] CO_2-TPD.

Fig. 5. (a) NH3-TPD profiles and (b) CO2-TPD profiles.

The NH_3-TPD and the CO_2-TPD can be used to investigate the total acidity and basicity of the catalysts, respectively as also shown in Table 3. The NH_3-TPD and CO_2-TPD profiles are also displayed in Fig. 5(a) and Fig. 5(b), respectively. It indicated that all catalysts mainly contained strong acid and strong basic. It notices that C and 4%Co/C samples show similar total acidity to the total basicity value (ca. 1.50), whereas the 6%Co/C catalyst exhibited lower total acidity to the total basicity value of 1.38.
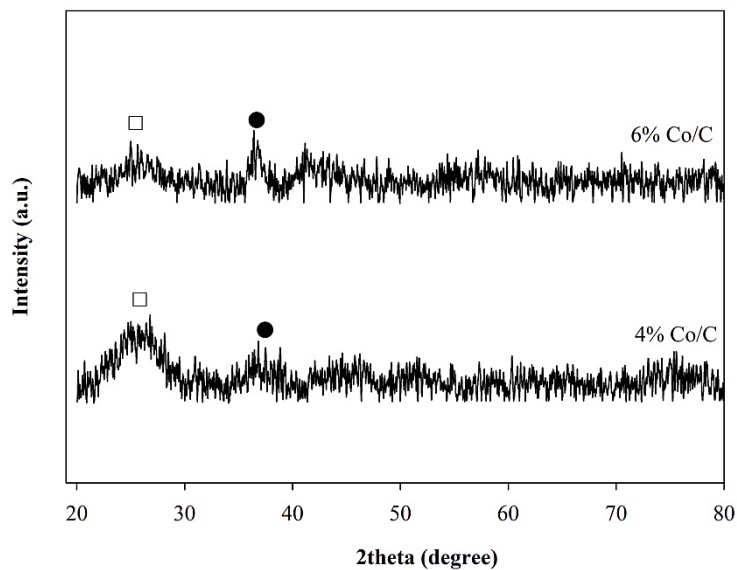

Fig. 6. X-ray diffraction patterns of cobalt catalysts. Legend: (□) graphite; (●) Co_3O_4.

XRD patterns of the activated carbon-supported Co catalysts are shown in Fig. 6. There are broad diffraction peak around $2\theta=22.5$, which can be assigned to the amorphous carbon composed of aromatic carbon sheets [24]. The XRD peak of Co_3O_4 was slightly observed at 36.8^o, while the CoO peak at 42.5^o was not evidently detected [14]. So, it appears that the 4%Co/C has Co oxide species (Co_3O_4 and CoO) in highly dispersed form.
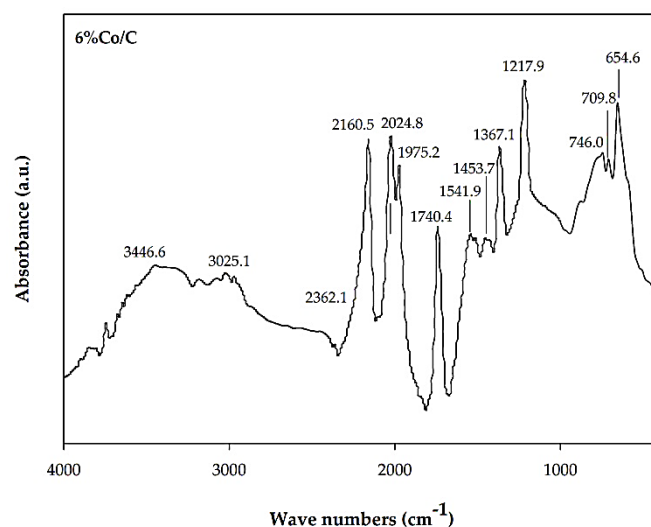
Fig. 7.   A typical FTIR spectrum of Co/C catalyst.

Table 4.   Functional group of activated carbons [25-28].

Catalysts	Assignment	Remark	Wave number (cm^{-1})
All catalysts	C≡C	Alkyne groups	2362, 2160
	C=C asymmetric stretch	Alkene groups	2024
	C=C asymmetric stretch	Alkene groups	1975
	C=O stretching	Carboxylic acids	1741
	C-Cl	Alkyl Halide	717
	O-H	Hydroxyl group	654
C	O-H stretching	Hydroxyl group as alcohol	3746
	C-H stretching	Quinones	2970
	C-O or C-OH	Ethers or phenolic groups	1365
	C-O or C-OH	Ethers or phenolic groups	1206
	C-O or C-OH	Ethers or phenolic groups	1006
	C-H	Benzene derivaties	740
4%Co/C	-	Cyclic amides or pyridine-like groups	1510
	C-O or C-OH	Ethers or phenolic groups	1013
6%Co/C	O-H stretching	Hydroxyl group as alcohol	3447
	C-H stretching	Carboxylic acids	3025
	-	Cyclic amides or pyridine-like groups	1542
	-	Nitro groups	1454
	C-O or C-OH	Ethers or phenolic groups	1367
	C-O or C-OH	Ethers or phenolic groups	1218
	γ (C–H) vibration	Benzene derivaties	746

FT-IR spectroscopy is a common technique used to analyze the functional groups in the catalyst samples. Table 4 and Fig. 7 display FT-IR results of catalysts. All catalysts show the visible band in range of 600-3800 cm^{-1}. All catalysts have alkyne, alkene carboxylic and alkyl halide groups which associated with the acid of catalysts.

In fact, carboxylic is strong acidic, while phenol, quinone and ether are weak acid [29]. Moreover, alkyl halide is a Lewis acid. In contrast, cyclic amides, pyridine-like groups and nitro groups are basic groups [29]. It appears that the result from FT-IR is consistent with the total acidity and the total basicity obtained using NH_3-TPD and CO_2-TPD methods.
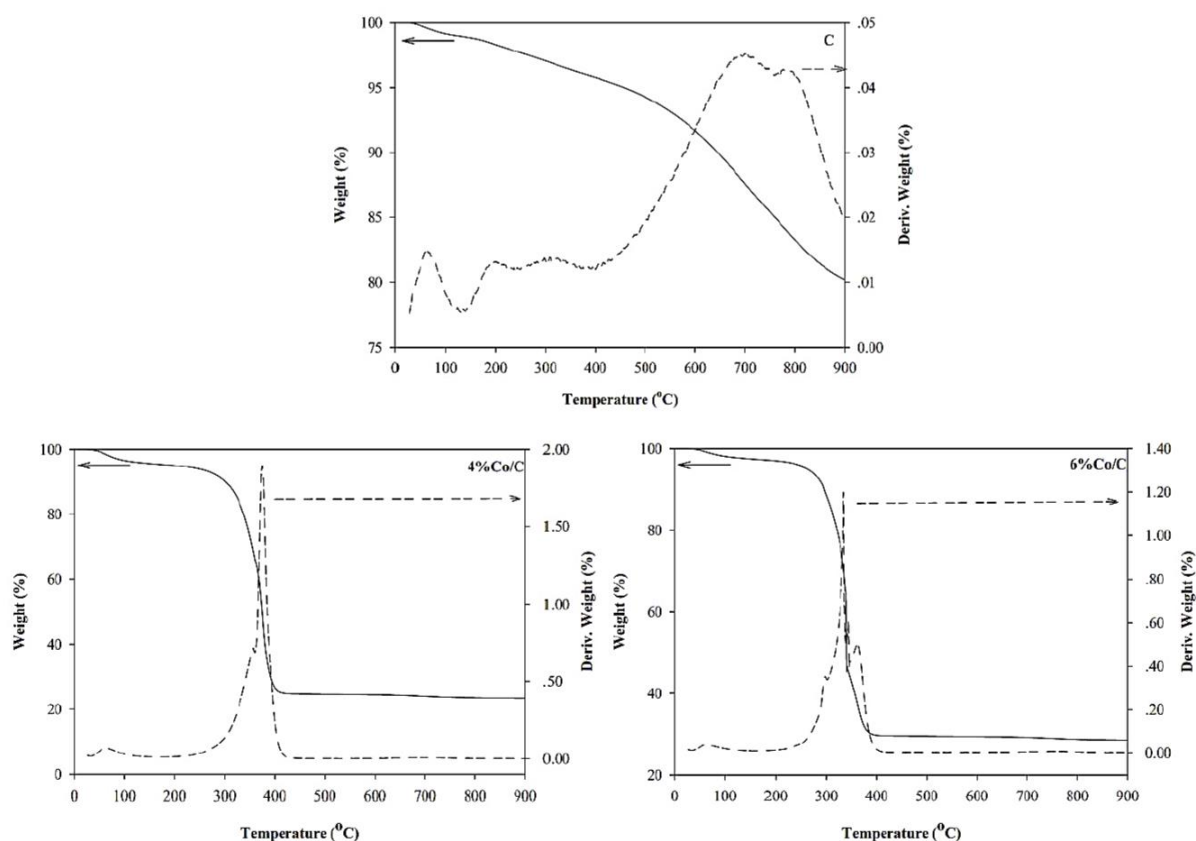
Fig. 8.   Thermal analysis of all catalysts.

Thermogravimetric results of all catalysts are presented in Fig. 8. For both Co/C catalysts, the mass loss during the thermogravimetric analysis can be separated into 3 stages [18]. The initial mass loss for temperature up to 250°C can be attributed to moisture elimination. The second stage is found at 250–400 °C range indicating the decomposition of organic materials that has a great mass loss (~70%). These results are also in agreement with other researchers [18]. While the mass of C catalyst was gradually decreased throughout the range of temperature that has a little mass loss about 20%.

3.2. Catalyst Testing

Fig. 9 shows the steady-state conversion of ethanol for each temperature on activated carbon and activated carbon-supported Co catalysts. In addition, ethanol conversion and acetaldehyde yield for all catalysts are shown in Table 5 and Fig. 10. As expected, ethanol conversion increases with increasing in reaction temperature because of its endothermic reaction. According to the literature, ethanol decomposition causes to ethylene and diethyl ether by dehydration method and acetaldehyde by dehydrogenation method. The reaction of dehydrogenation takes place in a coincident presence of Lewis base and acid sites, while that of dehydration conducts only acid sites [29]. Outcomes of the catalytic reaction test in this study certified that all activated carbons performed as catalysts of ethanol dehydrogenation, but in different activity. For temperature 250-350°C, it is certainly seen that all carbon catalysts show the similar activity. At temperature of 400°C, the C and 4%Co/C catalysts display high ethanol conversion about 48% and 54%, respectively. For 4% cobalt adding, to improve the activity of activated carbon catalyst by slightly increased the ethanol conversion from 48% to 54% while the same selectivity of acetaldehyde. As related with other study [14], adding cobalt to carbon catalyst can increased the ethanol conversion from 74% to 79%. While the impregnated 6% of Co, the ethanol conversion decreased rapidly about 18%. This may be caused by agglomeration and pore blockage.

During the ethanol dehydrogenation, it was found that all activated carbons exhibited the very high selectivity of acetaldehyde (higher than 90%), which was consistent with other studies [28, 30]. Moreover, Perez-Cadenas *et al.* [31] reported that chlorination causes to expanded acidity of Lewis acid sites on the activated carbon, but on the other side, it decreases Bronsted acid sites. In addition, our results show that the C and the 4%Co/C have the high total acidity to total basicity. So, it can be active for dehydrogenation of ethanol.
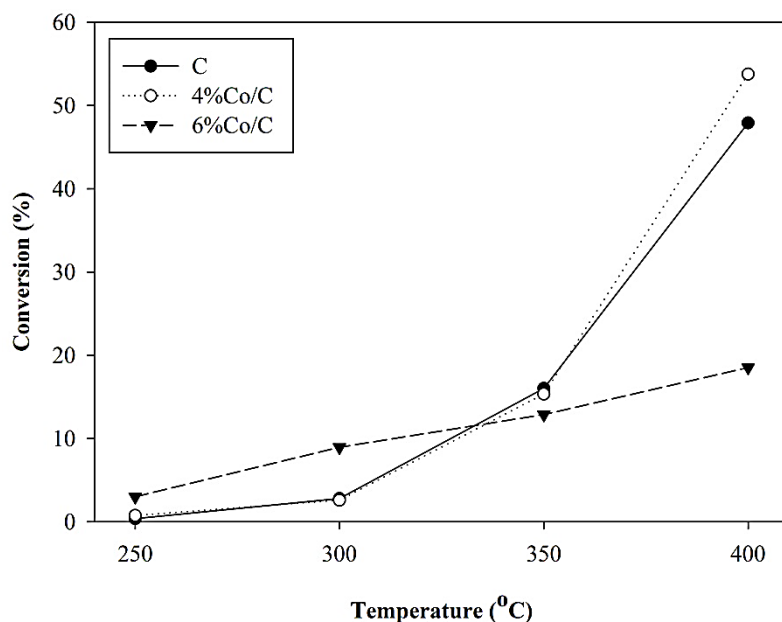

Fig. 9.   Ethanol conversion of activated carbon-supported Co catalysts.
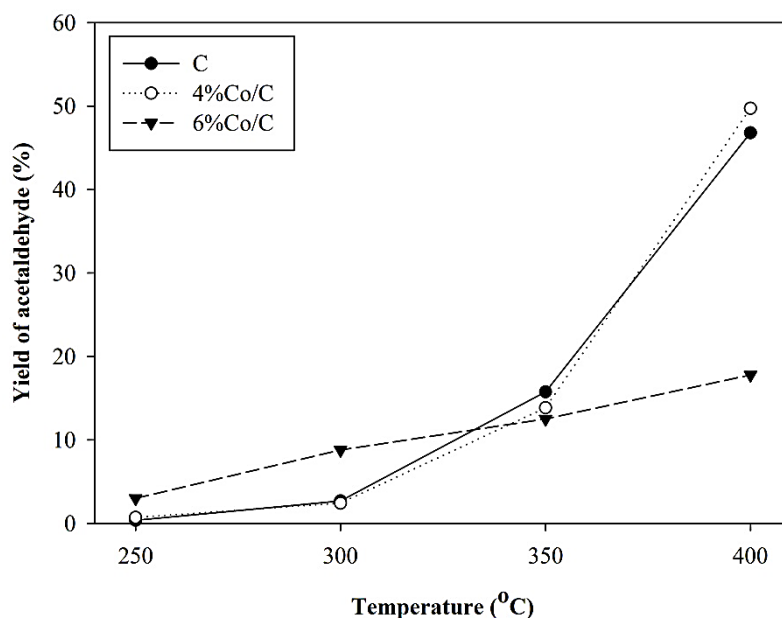

Fig. 10. Acetaldehyde yield of activated carbon-supported Co catalysts.

Table 5.   Ethanol conversion and acetaldehyde yield for activated carbon-supported Co catalysts.

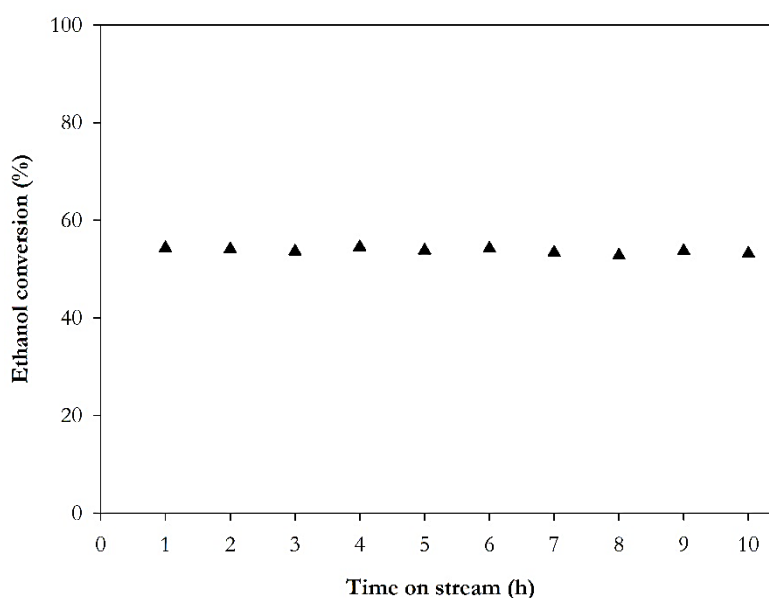| Samples	Temperatures (^{o}C)	C_2H_5OH conversion (%)	CH_3CHO yield (%)
C	250	0.37	0.36
	300	2.78	2.69
	350	16.02	15.75
	400	47.92	46.80
4%Co/C	250	0.74	0.71
	300	2.59	2.42
	350	15.34	13.84
	400	53.78	49.73
6%Co/C	250	2.99	2.99
	300	8.93	8.78
	350	12.87	12.50
	400	18.51	17.78

Fig. 11. Stability test for 4%Co/C catalyst at reaction temperature of 400°C.

The comparison of catalytic performance of activated carbon-supported Co catalysts in this work and Co-promoter on Cu/carbon commercial catalyst was considered [14]. It revealed that the best catalyst in this work had surface area of 727 m²/g and gained 54% of ethanol conversion with acetaldehyde yield of 50% at 400°C in ethanol dehydrogenation reaction, whereas the bimetallic Co-Cu on carbon catalyst showed surface area 986 m²/g having ethanol conversion about 78.5 % at the same temperature in oxidative ethanol dehydrogenation reaction. Although the catalyst in this work exhibits lower ethanol conversion and acetaldehyde yield, it is still competitive since the dehydrogenation undergoes without the introduction of oxygen.

Finally, the stability test of the 4%Co/C catalyst under time on stream of 10 h was carried out at 400°C. The stability result is displayed in Fig. 11. The ethanol conversion is continuously constant within 10 h of reaction indicating that this catalyst is quite stable under the specified reaction condition [11].

4. Conclusion

In summary, the study displayed that 4 wt% of Co impregnated on activated carbon, led to slightly increased activity of ethanol dehydrogenation having 54% conversion of ethanol (from 48%) and 50% yield of acetaldehyde (from 47%) at 400°C. This catalyst has the acidity to the basicity similar the activated carbon (~1.50). However, 6% of Co doped on activated carbon caused sample to pore blockage with some

agglomeration. This resulted in a decrease of the acidity to the basicity to 1.38. Therefore, it exhibited low activity of this reaction by 19% of ethanol conversion. In addition, all Co/C catalysts show very high selectivity to acetaldehyde (more than 90%) and undergo via dehydrogenation without introduction of oxygen.

Acknowledgments

References

[1] H. Idriss and E. G. Seebauer, "Reactions of ethanol over metal oxides," *Journal of Molecular Catalysis A.: Chemical*, vol. 152, pp. 201-212, 2000.

[2] J. E. Baker, R. Burch, and S. E. Golunski, "Synthesis of higher alcohols over copper/cobalt catalysts influence of preparative procedures on the activity and selectivity of Cu/Co/Zn/Al mixed oxide catalysts," *Applied Catalysis*, vol. 53, pp. 279-297, 1989.

[3] S. Tayrabekova, P. Maki-Arvela, M. Peurla, P. Paturi, K. Eranen, G. E. Ergazieva, A. Aho, D. Y. Murzin, and K. Dossumov, "Catalytic dehydrogenation of ethanol into acetaldehyde and isobutanol using mono- and multicomponent copper catalysts," *Comptes Rendus Chimie*, vol. 21, pp. 194-209, June 2018.

[4] E. Santacesaria, G. Carotenuto, R. Tesser, and M. Di Serio, "Ethanol dehydrogenation to ethyl acetate by using copper and copper chromite catalysts," *Chemical Engineering Journal*, vol. 179, pp. 209–220, Oct. 2011.

[5] S. Fujita, N. Iwasa, H. Tani, W. Nomura, M. Arai, and N. Takesawa, "Dehydrogenation of ethanol over Cu/ZnO catalysts prepared from various coprecipitated precursors," *Reaction Kinetic, Mechnisms and Catalysis*, vol. 73, no. 2, pp. 367-372, May 2001.

[6] J. M. Church and H. K. Joshi, "Acetaldehyde by dehydrogenation of ethyl alcohol," *Industrial and Engineering Chemistry*, vol. 43, no. 8, pp. 1804-1811, Aug. 1951.

[7] K. Pinkaew, O. Mekasuwandumrong, J. Panpranot, A. Shotipruk, P. Praserthdam, J. G. Goodwin, and B. Jongsomjit, "Zirconia modification on nanocrystalline titania supported cobalt catalysts for methanation," *Engineering Journal*, vol. 16, no. 4, pp. 29-37, July. 2012.

[8] J. Kruatim, S. Jantasee, and B. Jongsomjit, "Improvement of cobalt dispersion on Co/SBA-15 and Co/SBA-16 catalysts by ultrasound and vacuum treatments during post-impregnation step," *Engineering Journal*, vol. 21, no. 1, pp. 17-28, Jan. 2017.

[9] A. Ashok, A. Kumar, R. Bhosale, M. A. S. Saad, F. Almomani, and F. Tarlochan, "Study of ethanol dehydrogenation reaction mechanism for hydrogen production on combustion synthesized cobalt catalyst," *International Journal of Hydrogen Energy*, vol. 42, pp. 23464-23473, Feb. 2017.

[10] Z. Zhao, T. Bao, Y. Zeng, G. Wang, and T. Muhammad, "Efficient cobalt–manganese oxide catalyst deposited on modified AC with unprecedented catalytic performance in CO preferential oxidation," *Catalysis Communications*, vol. 32, pp. 47–51, Dec. 2012.

[11] R. S. Cruz, A. J. S. Mascarenhas, and H. M. C. Andrade, "Co-ZSM-5 catalysts for N_2O decomposition," *Appl. Catal. B Environ.*, vol. 18, no. 3-4, pp. 223-231, Oct. 1998.

[12] J. M. Church and H. K. Joshi, "Acetaldehyde by dehydrogenation of ethyl alcohol," *Industrial and Engineering Chemistry*, pp. 1804-1811, Aug. 1951.

[13] H. Zhou, J. Y. Wang, X. Chen, C. L. O'Young, and S. L. Suib, "Studies of oxidative dehydrogenation of ethanol over manganese oxide octahedral molecular sieve catalysts," *Microporous and Mesoporous Materials*, vol. 21, pp. 315-324, Jan. 1998.

[14] E. A. Sales, T. R. O. Souza, R. C. Santos, and H. M. C. Andrade, "N_2O decomposition coupled with ethanol oxidative dehydrogenation reaction on carbon-supported copper catalysts promoted by palladium and cobalt," *Catalysis Today*, vol. 107-108, pp. 114-119, Aug. 2005.

[15] J. Bedia, J. M. Rosas, J. Rodriguez-Mirasol, and T. Cordero, "Pd supported on mesoporous activated carbons with high oxidation resistance as catalysts for toluene oxidation," *Applied Catalysis B: Environmental*, vol. 94, pp. 8–18, Oct. 2009.

[16] M. L. Sekirifa, M. Hadj-Mahammed, S. Pallier, L. Baameur, D. Richard, and A. H. Al-Dujaili, "Preparation and characterization of an activated carbon from a date stones variety by physical activation with carbon dioxide," *Journal of Analytical and Applied Pyrolysis*, vol. 99, pp. 155–160, Oct. 2012.

[17] I. K. Erabee, A. Ahsan, A. W. Zularisam, S. Idrus, N. N. N. Daud, T. Arunkumar, R. Sathyamurthy, and A. E. Al-Rawajfeh, "A new activated carbon prepared from sago palm bark through physiochemical activated process with zinc chloride," *Engineering Journal*, vol. 21, no. 5, pp. 1-14, Sep. 2017.

[18] B. Niticharoenwong, A. Shotipruk, O. Mekasuwandumrong, J. Panpranot, and B. Jongsomjit, "Charasteristics of activated carbons derived from deoiled rice from rice bran residues," *Chemical Engineering Communications*, vol. 200, no. 10, pp. 1309-1321, Mar. 2013.

[19] C. Tangsathitkulchai, S. Junpirom, and J. Katesa, "Comparison of kinetic models for CO_2 gasification of coconut-shell chars: Carbonization temperature effects on char reactivity and porous properties of produced activated carbons," *Engineering Journal*, vol. 17, no. 1, pp. 13-27, Jan. 2013.

[20] M. Tangsathitkulchai, C. Tangsathitkulchai, K. Wongsooksin, and S. Chuyingsakuntip, "Removal of residual aluminium-dye complex and aluminium ion from spent natural-dye solution using activated carbons," *Engineering Journal*, vol. 16, no. 5, pp. 29-43, Oct. 2012.

[21] C. Krutpijit and B. Jongsomjit, "Catalytic ethanol dehydration over different acid-activated montmorillonite clays," *Journal of Oleo Science*, vol. 65, no. 4, pp. 347-355, Dec. 2015.

[22] T. Kamsuwan and B. Jongsomjit, "A comparative study of different Al-based solid acid catalysts for catalytic dehydration of ethanol," *Engineering Journal*, vol. 20, no. 3, pp. 63-75, Aug. 2016.

[23] S. J. Gregg and K. S. W. Sing, "Introduction," in *Adsorption, Surface Area and Porosity*, 2nd ed. New York: Academic Press Inc, 1982, pp. 3-5.

[24] M. Kitano, K. Arai, A. Kodama, T. Kousaka, K. Nakajima, S. Hayashi, and M. Hara, "Preparation of a sulfonated porous carbon catalyst with high specific surface area," *Catalysis Letters*, vol. 131, no. 1-2, pp. 242-249, June 2009.

[25] A. C. Lua and T. Yang, "Effect of activation temperature on the textural and chemical properties of potassium hydroxide activated carbon prepared from pistachio-nut shell," *Journal of Colloid and Interface Science*, vol. 274, pp. 594-601, Dec. 2003.

[26] K. Vikulov, S. Coluccia, and G. Martra, "Fourier-transform infrared spectroscopic studies of the adsorption of ketene on silica," *Journal of the Chemical Society, Faraday Transactions*, vol. 89, no. 7, pp. 1121-1125, 1993.

[27] M. S. Shafeeyan, W. M. A. W. Daud, A. Houshmand, and A. Shamiri, "A review on surface modification of activated carbon for carbon dioxide adsorption," *Journal of Analytical and Applied Pyrolysis*, vol. 89, pp. 143-151, Aug. 2010.

[28] W. T. Tsai, C. Y. Chang, M. C. Lin, S. F. Chien, H. F. Sun, and M. F. Hsieh, "Adsorption of acid dye onto activated carbons prepared from agricultural waste bagasse by $ZnCl_2$ activation," *Chemosphere*, vol. 45, pp. 51-58, Dec. 2010.

[29] J. Jasinska, B. Krzyzynska, and M. Kozlowski, "Influence of activated carbon modifications on their catalytic activity in methanol and ethanol conversion reactions," *Central European Journal of Chemistry*, vol. 9, no. 5, pp. 925-931, June 2011.

[30] F. Carrasco-Marin, A. Mueden, and C. Moreno-Castilla, "Surface-Treated Activated Carbons as Catalysts for the Dehydration and Dehydrogenation Reactions of Ethanol," *J. Phys. Chem. B.*, vol. 102, pp. 9229-9244, June 1998.

[31] A. F. Perez-Cadenas, F. J. Maldonado-Hodar, and C. Moreno-Castilla, "On the nature of surface acid sites of chlorinated activated carbons," *Carbon*, vol. 41, pp. 473-478, Oct. 2002.